Materials Advances

ROYAL SOCIETY OF CHEMISTRY

PAPER

View Article Online
View Journal | View Issue

Cite this: *Mater. Adv.*, 2024, 5, 1667

Synergy between activated carbon and ZnO: a powerful combination for selective adsorption and photocatalytic degradation

Wided Salah,[a] Wahid Djeridi,[b] Ammar Houas[a] and Leila Elsellami*[a]

Doping activated carbon with ZnO offers a compelling water treatment solution. Chemically synthesized using H_3PO_4 as an activating agent, the resulting composite material (AC/ZnO) showcases intriguing characteristics in terms of structure, specific surface, and ZnO localization on the carbon surface compared to pure activated carbon. These factors are crucial for the dual functionality of AC/ZnO in adsorption and photo-degradation of organic pollutants, such as phenol and formic acid. Empirical results reveal a significant enhancement in phenol adsorption by the AC/ZnO composite, achieving exceptional performance with 100% adsorption efficiency in just 2 hours. However, a noticeable performance drop occurs during formic acid adsorption, indicating the remarkable selectivity of AC/ZnO toward aromatic molecules, a novel finding. Evaluation of photocatalytic activity under UV irradiation demonstrates the synthetic AC/ZnO composite's high efficacy. ZnO incorporation significantly boosts the composite's ability to degrade formic acid compared to pure AC, achieving complete degradation within 240 minutes. This grants the material the advantage of auto-regeneration and reuse over four consecutive cycles, affirming its stability and lack of noticeable deactivation. The successful implementation of dual adsorption/photo-degradation functionality in the AC/ZnO composite underscores its efficacy. Consequently, even if a molecule lacks affinity for the activated carbon surface, it undergoes inevitable degradation in the presence of light.

Received 25th December 2023,
Accepted 30th December 2023

DOI: 10.1039/d3ma01171b

rsc.li/materials-advances

1. Introduction

The global water crisis is a major concern with widespread consequences. The growing scarcity of freshwater and the decreasing water resources have profound effects on the environment, agriculture, drinking water supply, and public health.[1] The factors underlying water shortage include, among other things, population growth, climate change effects, and environmental deterioration.[2,3]

Faced with these challenges, innovative solutions have been deployed to mitigate water scarcity, such as flocculation, sedimentation, ion exchange, adsorption, and membrane processes.[4–6] However, each water treatment method has its own limitations in terms of purification efficiency and applicability, notably high costs, as well as insufficient ability to remove certain pollutants.

Thus, it is imperative to develop effective and reliable methods and materials to purify contaminated waters in order to advance research. Even though adsorption is still a very effective method, it does not address the issue of the destruction of molecules adsorbed on the surface of materials.[7–9] To overcome this problem, the combination of adsorption and photocatalysis proves to be a promising strategy for creating even more efficient water treatment processes.

Moreover, the development of high-performance and reusable materials for adsorption and photocatalysis is of paramount importance.[10–12] Thus, the use of such a catalyst support as activated carbon, which is associated with TiO_2 or ZnO, makes it possible to efficiently merge these two treatment processes of the pollutants. In addition, the preparation methods of these composite materials exert a significant influence on the morphology, structure, and porous texture of these materials, which are essential attributes in order to achieve the desired performance.

Many studies have been published in this context. For instance, in 2005, Shon *et al.*[13] explored the synergy between adsorption and photocatalysis for the treatment of persistent organic pollutants in wastewater. The exclusive use of photocatalysis revealed an initial reverse reaction while using TiO_2 as

[a] *Laboratoire de Recherche Catalyse et Matériaux pour l'Environnement et les Procédés LRCMEP (LR19ES08), Faculté des Sciences de Gabès/Université de Gabès, Campus Universitaire Cité Erriadh, 6072 Gabès, Tunisia. E-mail: elsellami_leila@yahoo.fr*

[b] *Research Laboratory: Engineering Process and Industrial Systems, National School of Engineers of Gabes, University of Gabes, St Omar Ibn Elkhattab, 6029 Gabès, Tunisia*

a catalyst. They investigated the effect of adsorption pretreatment with powdered activated carbon (PAC) on photocatalysis. The results indicated that the simultaneous conjunction of PAC and TiO_2 eliminated the reverse reaction while improving organic removal.

In 2017, Li *et al.*[14] focused on the synthesis of nanostructured porous composites TiO_2/activated carbon fiber felt (TiO_2/ACFF) with the aim of studying their structure, morphology, and synergistic adsorption–photodegradation mechanism for toluene removal. Their research revealed that porous TiO_2/ACFF composites, by combining synergistic adsorption and photocatalytic capabilities, exhibit strong potential for toluene removal.

Recently, in his study, Thambiliagodage (2022)[15] has examined the joint application of TiO_2 with activated carbon, carbon nanotubes, graphene derivatives and g-C_3N_4 for the degradation of various pollutants present in water. These contaminants included dyes, pesticides, pharmaceuticals, phenols and heavy metals. He thoroughly assessed the inherent advantages and disadvantages of using each carbon-based material while addressing the challenges and opportunities associated with all of these materials.

Similarly, the study conducted by Alwadai *et al.* in 2023[16] explored the use of TiO_2 and AC-doped TiO_2 for the photocatalytic degradation of Rhodamine B (RhB) dye in wastewater treatment. This research analyzed several parameters including pH, initial dye concentration, trapping agents, kinetic properties and reusability. The main objective was to determine the optimization conditions in order to reduce energy consumption while maximizing the degradation rate.

It is notable that the majority of research studies have focused on the development of composite materials combining activated carbon and TiO_2,[17–20] whereas only a few studies have been devoted to the combination of ZnO and activated carbon.[21] It is important to emphasize that ZnO activation by UV radiation presents an attractive alternative for water treatment compared to TiO_2.[22] Indeed, numerous studies have proved that ZnO stands out as a promising photocatalyst under UV light with a high photocatalytic capacity and a band gap greater than that of TiO_2.[23]

Currently, research mainly focuses on the adsorption of aromatic compounds while overlooking aliphatic molecules. In this context, our study aims at the successful synthesis of a composite material associating activated carbon with ZnO. Its adsorption capacity (in the dark) and degradation capacity (in the presence of UV) are compared to those of pure activated carbon using experiments involving solutions of phenol (an aromatic pollutant) and formic acid (an aliphatic pollutant). These results make it possible to bring out the performance of the materials developed during the study, thus helping to shed light on more efficient materials that are better adapted to current needs.

2. Experimental section

2.1. Chemicals and reagents

The zinc oxide (ZnO) used in this study was commercially procured. The pollutants selected for removal were phenol (hydroxybenzene) and formic acid (methanoic acid). All reagents were purchased from Sigma Aldrich and were used without prior purification.

2.2. Elaboration of AC and AC/ZnO materials

Activated carbon (AC) was synthesized from olive stones. The raw material was washed and dried before the activation procedure. The olive stones were then immersed in an aqueous solution of phosphoric acid (H_3PO_4) with a weight ratio of 3 : 1, respectively. The mixture was stirred for 9 hours at 110 °C. Subsequently, the impregnated and dried biomass was ground to form particles with a diameter of about 80 μm. Lastly, the obtained particle size powder was pyrolyzed under nitrogen at a temperature of 410 °C for 2 hours and 30 minutes to obtain pure AC.[24,25]

For the synthesis of the hybrid material, the raw material was activated after washing and drying using the activating agent H_3PO_4 with the desired proportion of zinc oxide (2% ZnO by mass). Then, the suspensions were evaporated in an oven at 110 °C for 9 hours. The impregnated, dry and ground samples were then pyrolyzed for 2 hours and 30 minutes at 410 °C in a calcination oven. The sample of the hybrid material containing the activated carbon doped with zinc oxide was called AC/ZnO. The preparation methods of these materials are summarized in Fig. 1.

2.3. Instrumental and analytical techniques for the characterization of AC and the AC/ZnO hybrid material

The adsorption and/or photocatalytic properties of AC and AC/ZnO depended on their structural and textural characteristics as well as on their chemical characteristics of their surface. Several instrumental techniques were used to characterize these materials. X-ray diffraction (XRD) analyses were performed using an Analytical X'Pert Pro MPD diffractometer.

Scanning electron microscopy (SEM) coupled with energy dispersive X-ray spectroscopy (EDS) analyses were carried out using Hitachi microscopes. The measurements were made using an Autosorb-Quantachrome-1, a volumetric gas

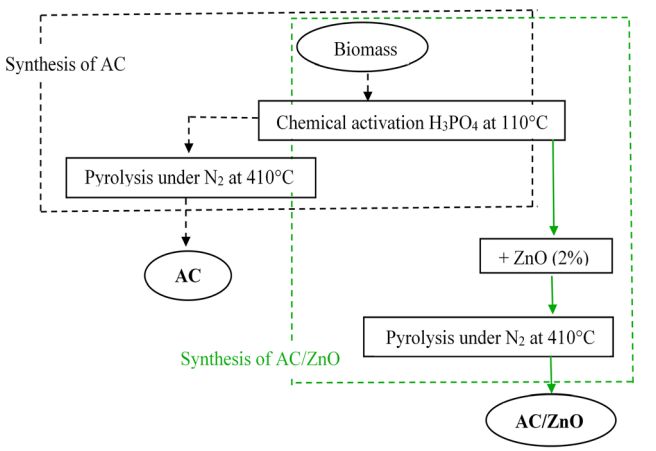

Fig. 1 Flowchart illustrating the synthesis procedure of activated carbon pure AC (left) and activated carbon doped with zinc oxide AC/ZnO (right).

adsorption apparatus of the SAP-LGC to determine the BET specific surface.

2.4. Experimental protocol

The adsorption and photocatalysis tests were first conducted in the dark and then under UV irradiation with reasonable durations for implementation in a sequential mode.

As regards the experiments on the adsorption kinetics of the pollutant (phenol or formic acid) on the material, a 100 mL reactor filled with 30 mL of pollutant solution at 20 mg L^{-1} was used. At time t = 0, 1 g of AC (doped or undoped with ZnO) was added into the reactor. Samples were subsequently taken at different times until the total adsorption or the concentration stabilization was reached. Each liquid sample taken was filtered through a syringe filter (pore diameter: 0.45 μm) before being analyzed.

On the other hand, when the lamp was switched on, the UV light was supposed to activate the ZnO present in the AC in order to trigger the degradation reactions of the pollutant. The UV rays were emitted by a Philips lampPL18 (365 nm) above the photo-reactor. At given time intervals, samples of approximately 0.7 mL of the polluted solution were removed. Then, the suspended particles were separated using 45 μm filters. A high-performance liquid chromatography instrument from Shimadzu HPLC was used in order to carry out the kinetic monitoring of adsorption and degradation.

3. Results and discussion

3.1. Crystal structure of AC and AC/ZnO materials

The structural investigation of AC/ZnO was performed by the XRD technique. Fig. 2 displays the XRD peaks of the synthesized sample. The diffractogram of pure AC is also included in this analysis for a better understanding of the results. These diffractograms made it possible to highlight the structural differences between ZnO-doped AC and undoped AC. Because of this approach, it was possible to characterize the crystalline structure of the AC/ZnO hybrid material more precisely and to better grasp the influence of ZnO on the structural properties of AC.

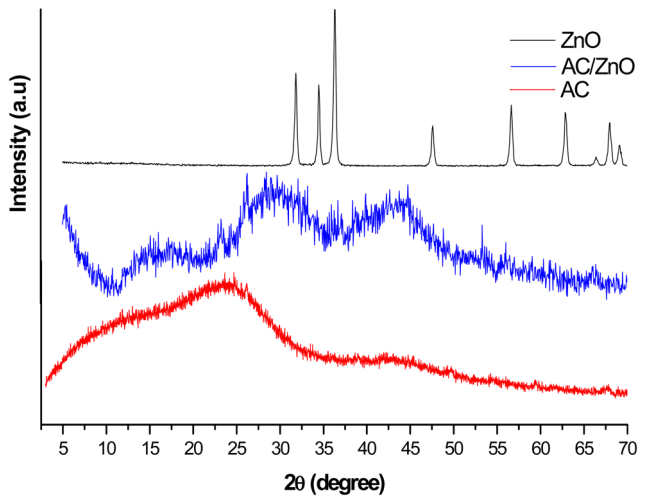

Fig. 2 X-ray diffractograms of the materials: activated carbon pure (AC), AC/ZnO composite material and ZnO.

The XRD profile of pure AC presents the characteristics of an amorphous carbonaceous material due to the absence of any identified graphitic carbon peak (Fig. 2). However, a crystal structure different from that of pure AC was observed after doping AC with ZnO (Fig. 2). These results clearly indicate that the fixation of ZnO in the AC matrix has a significant impact on its crystalline structure. Thus, it is demonstrated that the used synthesis method effectively enables the successful fixation of ZnO on the AC substrate. SEM analyses, however, were used to identify the AC/ZnO morphology.

3.2. Surface morphology of AC and AC/ZnO materials

Scanning electron microscopy (SEM) coupled with energy dispersive spectroscopy (EDS) was used to assess the surface morphology and elemental composition of the selected area. The SEM images of the AC and AC/ZnO samples are shown in Fig. 3.

Fig. 3A illustrates the SEM image of the AC sample, highlighting a very clean and irregular surface with a porous structure. This observation confirms the previous results which displayed the presence of numerous macropores in AC. It is worth noting that this macroporosity was added to the AC microporosity, which was not visible with SEM.

As for the SEM images of the AC/ZnO material presented in Fig. 3B, different scales were used to better understand the composite structure. The highlighted white area in the image is attributed to ZnO, whereas the gray and black areas refer to carbon. This observation confirms the successful fixation of ZnO on the AC surface and displays the distribution of these two materials in the composite structure.

It can be clearly observed in Fig. 3B that the ZnO particles come as agglomerates that are scattered among the large and small AC particles. The agglomeration of ZnO can be explained by the used synthesis method which consisted of introducing ZnO before the pyrolysis operation. In fact, in the case of AC/ZnO, the conversion of biomass to AC took place in the presence of ZnO, resulting in the imprisonment of the latter during the process of the AC network formation.

As regards the chemical nature, the EDS analysis of AC/ZnO surfaces revealed the presence of major chemical elements such as carbon, oxygen, phosphorus and zinc (Fig. 4 and Table 1). The significant contents of zinc and oxygen show that they were present in the form of zinc oxide. The presence of the chemical element (P) detected in EDS came from H_3PO_4 used for activation.

3.3. Study of the performance of the AC/ZnO material: adsorption and photodegradation of phenol and formic acid

The general framework of this paper aims to develop an AC/ZnO composite material capable of capturing two target pollutants, namely phenol and formic acid, by adsorption. In addition,

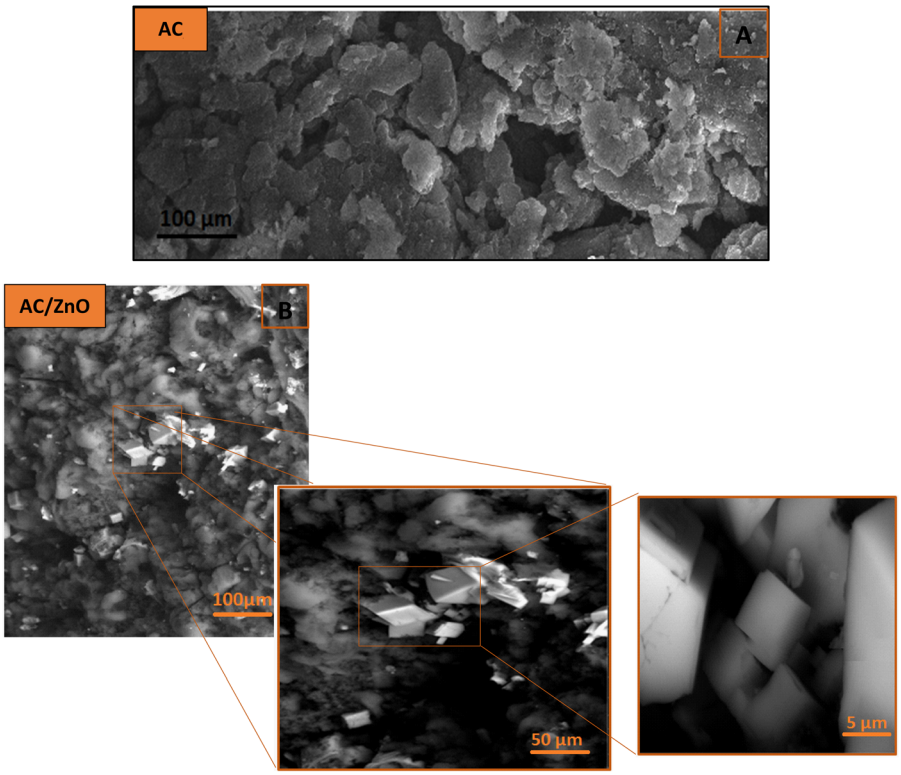

Fig. 3 SEM images of (A) activated carbon pure (AC) and (B) activated carbon doped with ZnO (AC/ZnO).

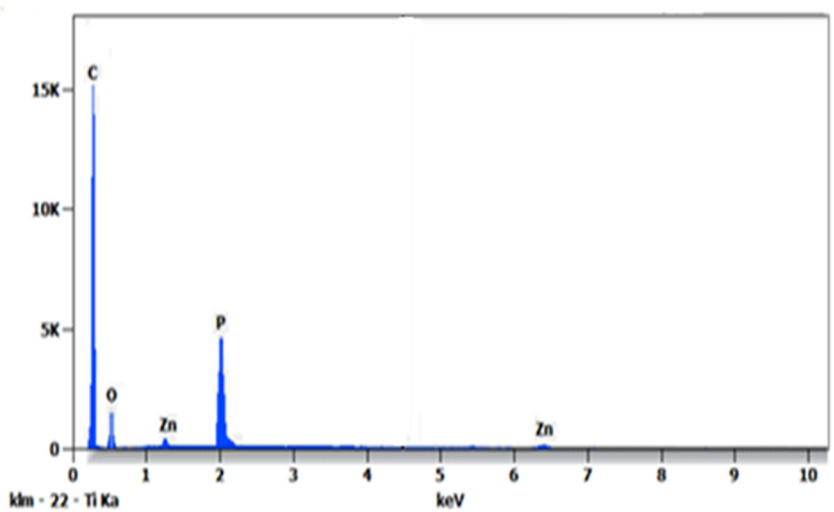

Fig. 4 EDS spectrum of the activated carbon/ZnO composite material (AC/ZnO).

the distinctive feature of this composite material is its ability to degrade these pollutants under the effect of UV light.

3.3.1. Comparison of adsorption capacities of the AC/ZnO composite material and AC. In order to evaluate the impact of doping AC with ZnO on the efficiency of the adsorption process, tests were carried out using the AC/ZnO composite material (98/2% respectively). Each experiment was conducted with a quantity equivalent to 1 g L^{-1} of AC/ZnO in the presence of an initial concentration of 20 mg L^{-1} of phenol or formic acid.

Empirical results have shown a significant improvement in the adsorption capacity of the AC/ZnO material in comparison with undoped AC. The AC/ZnO material reached a full adsorption capacity of the initial phenol concentration (20 mg L^{-1}) corresponding to a rate of 100% while pure AC only reached about 76% as shown in Fig. 5. Indeed, doping AC with ZnO led to an increase in the number of adsorption sites available at the surface of the material. This rise in the adsorption capacity of the composite material is strikingly original.

Table 1 Atom and compound percentages obtained from energy dispersive X-ray spectroscopy (EDS) of the AC/ZnO sample

Element	Atom (%)	Compound (%)
C	88.36	82.37
O	7.32	8.87
P	3.89	7.83
Zn	0.43	0.93
Total	100.00	100.00

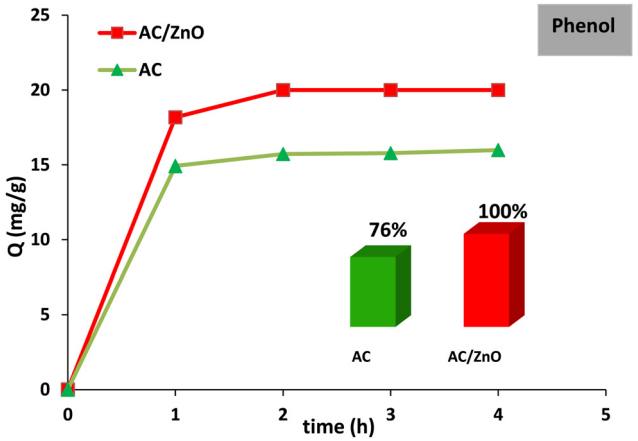

Fig. 5 Phenol adsorption kinetics in the presence of activated carbon pure (AC) and AC/ZnO composite material. [Phenol] = 20 mg L^{-1}.

Fig. 6 compares the adsorption capacities of AC and CA/ZnO to adsorb formic acid (FA). A very low percentage of adsorption (less than 0.6%) was observed, suggesting that the adsorption of FA by pure AC was mainly influenced by the structural properties of the adsorbent and the surface chemistry. Moreover, doping AC with ZnO did not seem to have a significant influence since AC/ZnO also had a poor adsorption capacity (less than 6.2%).

Fig. 7 schematically illustrates the mechanisms of phenol and FA adsorption on activated carbon aiming to explain these phenomena. Phenol is a molecule composed of a hydrophobic benzene ring to which a polar hydroxyl group (−OH) is

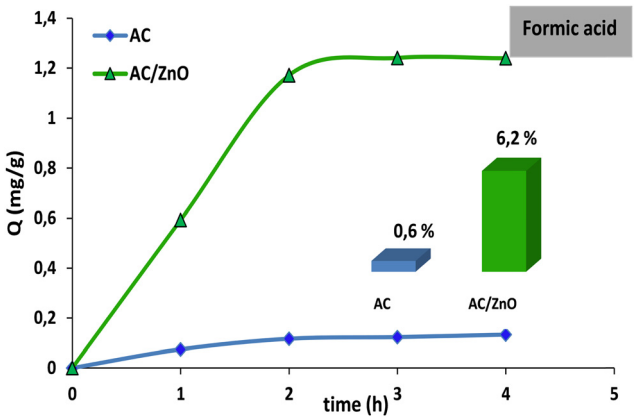

Fig. 6 Comparison of formic acid (FA) degradation using activated carbon pure (AC) and AC/ZnO composite material. [FA] = 20 mg L^{-1}.

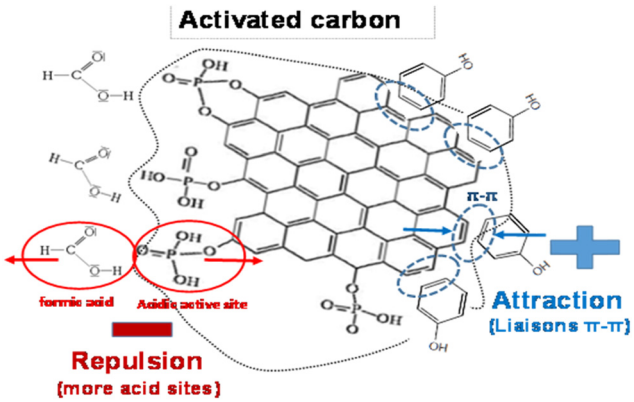

Fig. 7 Proposal schematic illustration of the adsorption of phenol and formic acid by pure activated carbon (AC).

attached. Even though the hydroxyl group gives phenol certain water solubility due to its polar character, the predominant benzene ring makes phenol generally hydrophobic.

However, the presence of the benzene ring resulted in a preferential interaction between the phenol molecules and the AC pi-bonds, thus forming hydrophobic aggregates rather than dispersing in water. Moreover, the process of fixing ZnO on AC created a positive effect, which mainly promoted physical interactions of van der Waals type between the aromatic nuclei of phenol molecules and the aromatic rings of AC, involving the delocalized π electrons.[26–28] This synergy between AC and ZnO made it possible to optimize the efficiency of the adsorption process, rendering the AC/ZnO composite material particularly promising for depolluting the water contaminated by aromatic compounds.

As for FA, the AC which was chemically treated by activation with H_3PO_4 had an increased amount of oxygenated groups such as carboxylic acids, quinones and anhydrides. Nevertheless, this increase in acid groups on the surface appeared to reduce interactions with FA molecules, thus explaining its inadequate adsorption capacity. Formic acid is a negatively charged organic acid molecule due to the presence of an acid group (HCOOH). This negative charge led to an interaction with the AC acid sites by electrostatic repulsive forces. These repulsive forces between the acid groups of AC and those of FA could alter the adsorption capacity of the material, thus making FA adsorption less efficient or less preferential than that of phenol.

Indeed, the results show that the differences in adsorption between phenol and FA mainly depend on the structural specificities resulting from the synthesis route, which leads to a selective power of the material. This selective power was presented by a variation in the quantity adsorbed between phenol and FA at equilibrium.

3.3.2. Comparative study of the photocatalytic activity of AC/ZnO material and AC. Fig. 8 and 9 show the disappearance profiles of phenol and FA in the presence of the AC/ZnO catalyst. Initially, the profiles were studied in the dark and then under UV irradiation. The adsorption and photodegradation curves of AC are also included for comparison in the two previously mentioned figures.

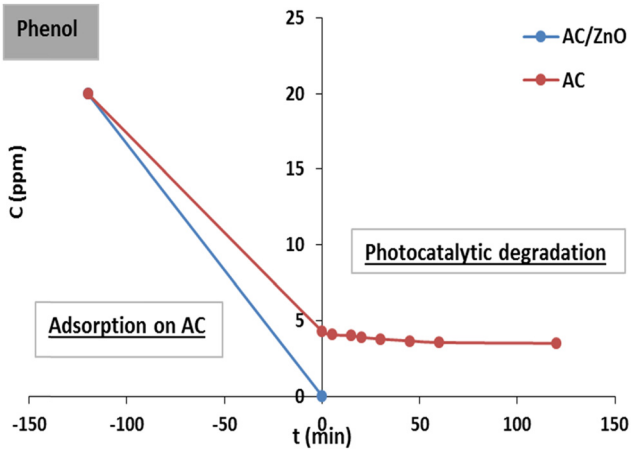

Fig. 8 Adsorption and photodegradation kinetics of phenol by activated carbon (AC) and AC/ZnO composite material. [Phenol] = 20 mg L^{-1}.

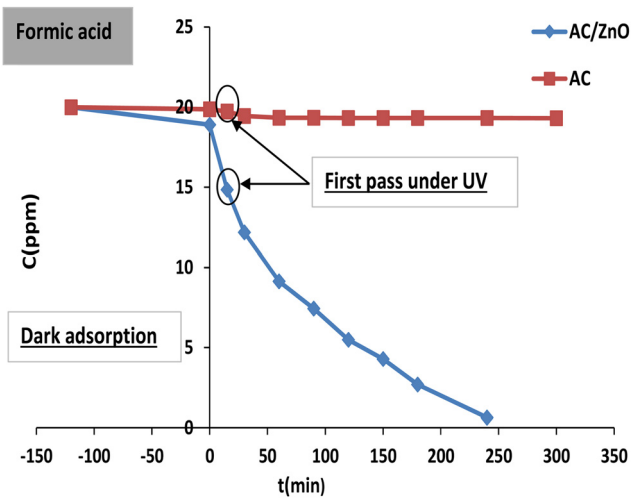

Fig. 9 Adsorption and photodegradation kinetics of formic acid (FA) by activated carbon (AC) and AC/ZnO composite material. [FA] = 20 mg L^{-1}.

It can be observed that the photocatalytic degradation process continued when the adsorption reached equilibrium. The time required for the maximum amount of pollutant in the solution to be adsorbed by the material was 2 hours. These data suggest that the presence of ZnO led to an increase in adsorption sites available in the AC network without affecting the time required to reach adsorption equilibrium.

It is worth noting once again that the adsorption rate of phenol was 100% before the irradiation phase, which caused total elimination of this pollutant in the presence of AC/ZnO in the adsorption phase.

On the other hand, more than 76% of the phenol adsorbed at equilibrium has already been eliminated for the treatment with AC. Then, under UV irradiation, AC did not show any phenol degradation. This behavior seems logical since AC was not a photoactive agent in the absence of the ZnO catalyst.

It is noticeable in Fig. 9 that the adsorption kinetic curves of AC and AC/ZnO are practically superimposed, demonstrating an almost horizontal appearance. These non-irradiated materials acted as simple adsorbents and were limited to low removal rates as shown in Fig. 6. For further treatment with AC, the change in FA concentration was negligible over time. Thus, the FA elimination kinetics obtained in the presence of light was practically identical to that obtained in its absence. As expected, only the adsorption phenomenon intervened in the elimination of FA when undoped AC was present.

However, the curve profile with AC/ZnO was distinguished by a significant drop in the FA concentration (20 mg L^{-1}) over time, reaching complete disintegration within 240 minutes under UV irradiation. This study demonstrates the possibility of combining ZnO with AC in order to give it an additional photocatalytic property without altering its initial adsorption capacity.

The proposed mechanism is illustrated in Fig. 10 for the irradiation phase. Once adsorbed on the material, FA molecules were eliminated and replaced either by (i) those present in the liquid or by (ii) those stored by AC (diffusion). Since ZnO needs light to become activated, a UV lamp was used as a light source to trigger the photocatalytic phenomenon. The heterogeneous photocatalytic reaction was based on the electron–hole pair production (as a result of the excitation of ZnO by UV) and followed by the formation of hydroxyl radicals ($OH^{\bullet}$).[29] These radicals then reacted with FA, mineralizing it into CO_2 and H_2O.[30] The adsorption–photocatalysis hybrid coupling using the AC/ZnO composite material significantly improved both the FA removal rate and the auto-regeneration of the material.

Knowing the order of the degradation reaction was essential for a better understanding of the phenomenon of the FA photocatalytic degradation. Accordingly, based on the results found in the literature, the following equation was applied to determine the order of the FA degradation kinetics:[31]

$$\mathrm{Ln}(C_0/C) = k_{app}\, t \quad (1)$$

Fig. 11 shows a variation of $\ln(C_0/C)$ *versus* time which follows an almost linear profile with first-order kinetics.

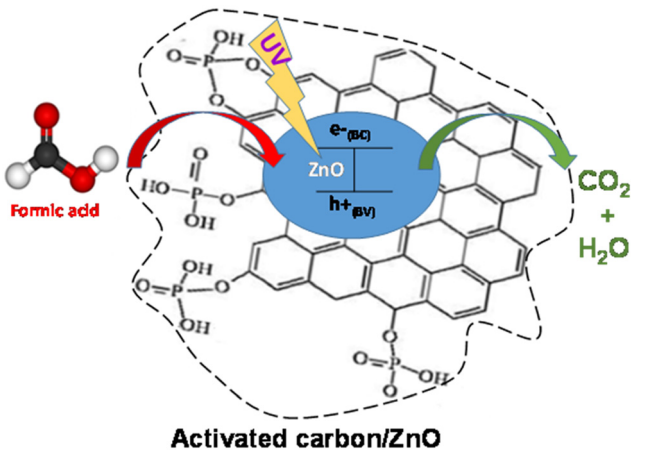

Fig. 10 Proposal schematic illustration of formic acid degradation and auto-regeneration of the activated carbon/ZnO composite material (AC/ZnO).

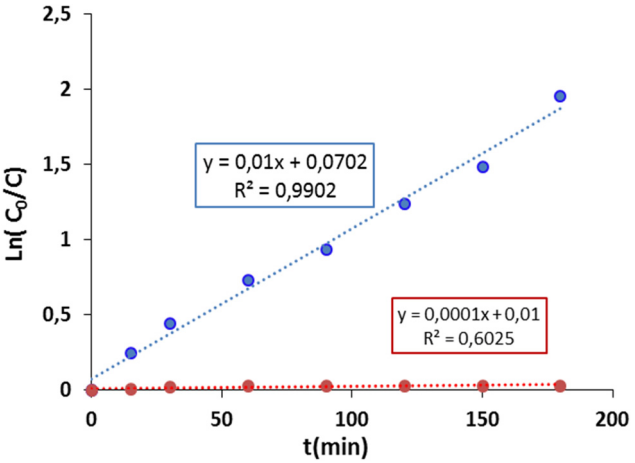

Fig. 11 Adjustments to the pseudo-first-order equation for the photodegradation of formic acid (FA) in the presence of AC/ZnO composite material. [FA] = 20 mg L^{-1}.

However, it is important to note that the best correlations (the highest R^2) indicate the Langmuir model. This suggests that the FA which disappeared in solution was mineralized.

The results illustrated in Fig. 11 show that ZnO is more efficient for the degradation of this type of pollutant. The rate constant obtained using AC/ZnO was 100 times greater than that obtained in the presence of pure AC (0.01 and 0.0001 mg L^{-1} min^{-1} respectively). Similarly, a degradation rate of more than 98% was recorded in the presence of AC/ZnO compared to 3% using AC after 4 hours under UV.

3.4. Normalization of quantities adsorbed by specific surface area: Impact and analysis

During the analytical comparison between the two types of adsorbents, namely pure AC and AC/ZnO, two distinct measurements of the adsorbed quantities were taken into account: the adsorbed quantities of phenol and FA on the one hand and the adsorbed quantities normalized by the specific surface area for the same compounds on the other hand. The results revealed a significant distinction between the two measurement approaches (Fig. 12).

As regards the non-normalized adsorbed amounts, the difference between pure AC and ZnO-doped AC was less pronounced. However, once the adsorbed quantities were normalized to neutralize the impact of specific surface area, a much more pronounced difference emerged. The normalized adsorbed quantities were found to be significantly higher for ZnO-doped AC compared with pure AC. Knowing that the surface area of AC (1014 m^2 g^{-1}) is high in comparison to that of ZnO-doped AC (950 m^2 g^{-1}).

This observation clearly suggests that the presence of ZnO exerts a positive effect on the adsorption of the compounds in question, thus overcoming the influence of the specific surface area. This confirms that ZnO plays a determining role in adsorption. This study deepens the understanding of the adsorption of these two pollutants on the AC/ZnO composite as well as on pure AC, thus highlighting the primordial

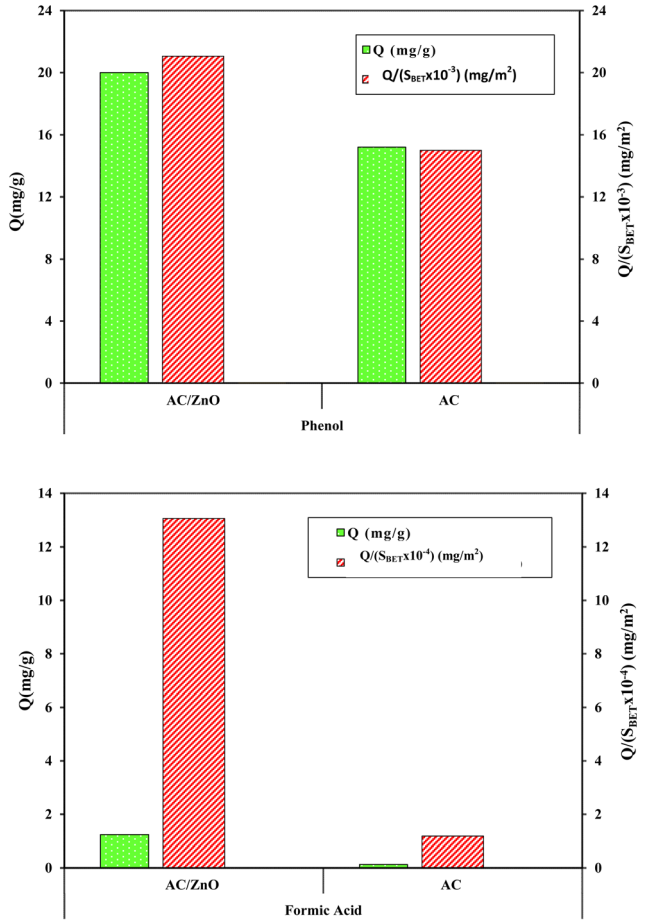

Fig. 12 Adsorbed quantities and adsorbed quantities normalized by specific surface of pure activated carbon (AC) and activated carbon doped with ZnO (AC/ZnO) for the two pollutants: phenol and formic acid. Concentration of pollutant Co: 20 mg L^{-1}.

importance of the presence of ZnO in this process. Indeed, ZnO is a dominant factor of the adsorption by the creation of active sites compared to the adsorption on the specific surface.

3.5. Formic acid elimination: auto-regeneration and reuse

This section focuses on the stability of the AC/ZnO material over four cycles, particularly its ability to remove FA by photocatalysis in the presence of UV light. The good performance recorded after the first use of the material shows its ability to auto-regenerate. Therefore, experiments have been carried out by alternating photocatalytic phases in order to guarantee its auto-regeneration and reuse.

There was almost no decrease in the degradation rate after 3 consecutive cycles as illustrated in Fig. 13, maintaining the FA degradation rate which was still 97%. This indicates that the photocatalytic material was not significantly deactivated and had good stability. At the fourth cycle, the degradation rate showed a slight decrease, suggesting that, with prolonged use, the AC/ZnO composite underwent a partial degradation of the active sites as they were reused and auto-regenerated. At the

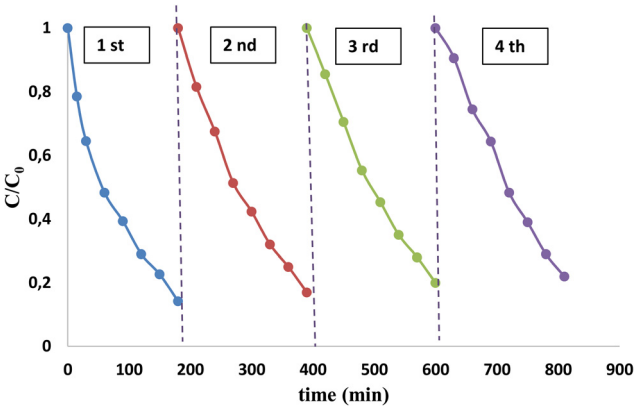

Fig. 13 Formic acid disappearance kinetics over four cycles using the AC/ZnO composite material under UV light. [FA] = 20 mg L^{-1}.

end of the photocatalytic tests, the composite still retained high photocatalytic and reuse capabilities despite a slight alteration of the active sites of the AC/ZnO material.

4. Conclusions

The bifunctional AC/ZnO material synthesized by chemical activation has been subjected to exhaustive evaluation in order to demonstrate its ability to remove two pollutants (phenol and FA) and its stability under repeated processing conditions. The main findings of this study are as follows:

• AC and AC/ZnO materials have been successfully developed using a chemical synthesis process, making them suitable for water treatment.

• A significant adsorption capacity played a favorable role in the effectiveness of the AC/ZnO material in eliminating almost all of the phenol present in a polluted solution at a concentration of 20 mg L^{-1} after a treatment of 2 hours in the dark. In contrast, the adsorption rate on pure AC was only 76%. These results highlight the importance of the AC/ZnO material in the fight against aromatic and aliphatic pollutants.

• The measured FA adsorption rates were found to be much lower than those of phenol for AC and AC/ZnO materials. This difference shows the specific adsorption selectivity of these materials for aromatic pollutants.

• The remarkable photocatalytic performance of the AC/ZnO material can be attributed to the optimal distribution of ZnO particles inside the carbon matrix. This distribution allows the efficient use of UV radiation and promotes a synergistic coupling between the adsorption and photocatalysis processes.

• The absence of significant degradation of phenol and FA on pure AC under UV irradiation highlights the crucial role of the ZnO catalyst in pollutant degradation.

• The satisfactory modeling of FA degradation on the AC/ZnO material by the Langmuir–Hinshelwood model confirms the relevance of this material for the degradation process.

• The AC/ZnO material maintained high stability and exhibited no noticeable deactivation with an FA degradation rate of up to 97% after four hours in three consecutive cycles.

The ultimate goal of this research was to develop a photocatalytic material that is both profitable and economically viable, thus opening up promising prospects for the effective treatment of contaminated water.

Conflicts of interest

There are no conflicts to declare.

References

1 E. Emmanuel, Y. Perrodin, G. Keck, J.-M. Blanchard and P. Vermande, Ecotoxicological risk assessment of hospital wastewater: a proposed framework for raw effluents discharging into urban sewer network, *J. Hazard. Mater.*, 2005, **117**, 1–11, DOI: 10.1016/j.jhazmat.2004.08.032.

2 B. F. Kim, R. E. Santo, A. P. Scatterday, J. P. Fry, C. M. Synk, S. R. Cebron, M. M. Mekonnene, A. Y. Hoekstra Saskia de Peeh, M. W. Bloema, R. A. Neffa and K. E. Nachman, Country-specific dietary shifts to mitigate climate and water crises, *Global Environ. Change*, 2020, **62**, 101926, DOI: 10.1016/j.gloenvcha.2019.05.010.

3 P. C. S. J. Laroche, C. J. E. Schulp, T. Kastner and P. H. Verburg, Telecoupled environmental impacts of current and alternative Western diets, *Global Environ. Change*, 2020, **62**, 102066, DOI: 10.1016/j.gloenvcha.2020.102066.

4 S. Rangabhashiyam, N. Anu and N. Selvaraju, Sequestration of dye from textile industry wastewater using agricultural waste products as adsorbents, *J. Environ. Chem. Eng.*, 2013, **1**, 629–641, DOI: 10.1016/j.jece.2013.07.014.

5 R. Malik, D. S. Ramteke and S. R. Wate, Adsorption of malachite green on groundnut shell waste based powdered activated carbon, *Waste Manage.*, 2007, **27**, 1129–1138, DOI: 10.1016/j.wasman.2006.06.009.

6 M. Kadhom, M. Al-Furaiji, S. Salih, M. A. Al-Obaidi, G. H. Abdullah and N. Albayati, A review on UiO-66 applications in membrane-based water treatment processes, *J. Water Process. Eng.*, 2023, **51**, 103402, DOI: 10.1016/j.jwpe.2022.103402.

7 W. Djeridi, A. Ouederni, A. D. Wiersum, P. L. Llewellyn and L. El Mir, High pressure methane adsorption on microporous carbon monoliths prepared by olives stones, *Mater. Lett.*, 2013, **99**, 184–187, DOI: 10.1016/j.matlet.2013.03.044.

8 T. Zhang, X. Zhang and H. Li, Kinetics and equilibrium study of phenol adsorption by activated carbonderived from pig blood, *Carbon Trends*, 2023, **12**, 100281, DOI: 10.1016/j.cartre.2023.100281.

9 W. Djeridi, A. Ouederni, N. Ben Mansour, P. L. Llewellyn, A. Alyamani and L. El Mir, Effect of the both texture and electrical properties of activated carbon on the CO2 adsorption capacity, *Mater. Res. Bull.*, 2016, **73**, 130–139, DOI: 10.1016/j.materresbull.2015.08.032.

10 J. Schneider, M. Matsuoka, M. Takeuchi, J. Zhang, Y. Horiuchi, M. Anpo and D. W. Bahnemann, Understanding TiO_2 photocatalysis: mechanisms and materials, *Chem. Rev.*, 2014, **114**, 9919–9986, DOI: 10.1021/cr5001892.

11 S. Singla, S. Sharma, S. Basu, N. P. Shetti and T. M. Aminabhavi, Photocatalytic watersplitting hydrogen production via environmental benign carbon basednanomaterials, *Int. J. Hydrogen Energy*, 2021, **46**, 33696–33717, DOI: 10.1016/j.ijhydene.2021.07.187.

12 M. R. K. Estahbanati, M. Feilizadeh, M. Shokrollahi Yancheshmeh and M. C. Iliuta, Effects of carbon nanotube and carbon sphere templates in TiO_2 composites for photocatalytic hydrogen production, *Ind. Eng. Chem. Res.*, 2019, **58**, 2770–2783, DOI: 10.1021/acs.iecr.8b05815.

13 H. K. Shon, S. Vigneswaran, H. H. Ngo and J.-H. Kim, Chemical coupling of photocatalysis with flocculation and adsorption in the removal of organic matter, *Water Res.*, 2005, **39**, 2549–2558, DOI: 10.1016/j.watres.2005.04.066.

14 M. Li, Bin Lu, Qin-Fei Ke, Ya-Jun Guo and Ya-Ping Guo, Synergetic effect between adsorption and photodegradation on nanostructured TiO_2/activated carbon fiber felt porous composites for toluene removal, *J. Hazard. Mater.*, 2017, **333**, 88–98, DOI: 10.1016/j.jhazmat.2017.03.019.

15 N. Alwadai, M. Shakil, U. Inayat, M. Tanveer, M. Ashraf, S. Sajid Ali Gillani, M. S. Al-Buriahi and Z. A. Alrowaili, Unlocking the synergistic potential of peanut shell derived activated carbon-doped TiO_2 for highly efficient photocatalytic removal of organic dye under visible light irradiation, *Mater. Sci. Eng. B*, 2023, **296**, 116646.

16 C. Thambiliagodage, Efficient photocatalysis of carbon coupled TiO_2 to degrade pollutants in wastewater – A review, *Environ. Nanotechnol. Monit. Manag.*, 2022, **18**, 100737, DOI: 10.1016/j.enmm.2022.100737.

17 G. Colón, M. C. Hidalgo and J. A. Navio, A novel preparation of high surface area TiO_2 nanoparticles from alkoxide precursor and using active carbon as additive, *Catal. Today*, 2002, **76**, 91–101, DOI: 10.1016/S0920-5861(02)00207-9.

18 E. Bu, X. Chen, C. Lopez-Cartes, F. Cazana, A. Monzon, J. Martínez-Lopez and J. J. Delgado, Effect of the TiO_2-carbon interface on charge transfer and ethanolphoto-reforming, *Catal. Today*, 2023, **422**, 114220.

19 A. Saha, A. Moya, A. Kahnt, D. Iglesias, S. Marchesan, R. Wannemacher, M. Prato, J. J. Vilatela and D. M. Guldi, Interfacial charge transfer in functionalized multi-walled-carbon nanotube@TiO_2 nanofibres, *Nanoscale*, 2017, **9**, 7911–7921, DOI: 10.1039/c7nr00759k.

20 S. Lettieri, V. Gargiulo, D. K. Pallotti, G. Vitiello, P. Maddalena, M. Alfe and R. Marotta, Evidencing opposite charge-transfer processes at TiO_2/graphene-related material-sinterface through combined EPR, photoluminescence and photocatalysisassessment, *Catal. Today*, 2018, **315**, 19–30, DOI: 10.1016/j.cattod.2018.01.022.

21 M. Samy, A. G. Kumi, E. Salama, M. ElKady, K. Mensah and H. Shokry, Heterogeneous activation of persulfate by a novel nano-magnetite/ZnO/activated carbon nanohybrid for carbofuran degradation: Toxicityassessment, water matrices, degradation mechanism and radical andnon-radical pathways, *Process Saf. Environ. Prot.*, 2023, **169**, 337–351, DOI: 10.1016/j.psep.2022.11.038.

22 L. Elsellami and W. Djeridi, Charge transfer modulation (e^-/h^+) between TiO_2, ZnO, and Ag for a superior photocatalytic performance, *J. Mater. Res.*, 2022, **37**, 897–908, DOI: 10.1557/s43578-022-00504-6.

23 M. Habibi, A. Habibi-Yangjeh, M. Sabri, H. Chand, V. Krishnan and C. Wang, Highly impressive activation of persulfate ions by novel ZnO/$CuCo_2O_4$nanostructures for photocatalytic removal of tetracycline hydrochloride under-visible light, *Environ. Technol. Innov.*, 2021, **24**, 102038.

24 W. Djeridi, N. Ben Mansour, A. Ouederni, P. L. Llewellyn and L. El Mir, Elaboration of porous carbon/nickel nanocomposites for selective gas storage, *Solid State Sci.*, 2019, **93**, 37–43, DOI: 10.1016/j.solidstatesciences.2019.05.003.

25 W. Djeridi, N. Ben Mansour, A. Ouederni, P. L. Llewellyn and L. El Mir, Study of methane and carbon dioxide adsorption capacity by synthetic nanoporous carbon based on pyrogallol-formaldehyde, *Int. J. Hydrogen Energy*, 2017, **42**, 8905–8913, DOI: 10.1016/j.ijhydene.2016.06.105.

26 A. Dąbrowski, P. Podkościelny, Z. Hubicki and M. Barczak, Adsorption of phenolic compounds by activated carbon—a critical review, *Chemosphere*, 2005, **58**, 1049–1070, DOI: 10.1016/j.chemosphere.2004.09.067.

27 T. Zhang, X. Zhang and H. Li, Kinetics and equilibrium study of phenol adsorption by activated carbonderived from pig blood, *Carbon Trends*, 2023, **12**, 100281, DOI: 10.1016/j.cartre.2023.100281.

28 C. Du, W. Feng, S. Nie, X. Su, H. Liu, J. Feng, J. Sun, C. Hu and S. Dong, π–π conjugation driving degradation of aromatic compounds with in-situ hydrogen peroxide generation over $Zn_2In_2S_5$ grown on nitrogen-doped carbon spheres, *Appl. Catal., B*, 2022, **310**, 121298, DOI: 10.1016/j.apcatb.2022.121298.

29 L. Elsellami, K. Sahel, F. Dappozze, S. Horikoshi, A. Houas and C. Guillard, Titania-based photocatalytic degradation of two nucleotide bases,cytosine and uracil, *Appl. Catal., A*, 2014, **485**, 207–213, DOI: 10.1016/j.apcata.2014.07.043.

30 L. Elsellami, F. Dappozze, N. Fessi, A. Houas and C. Guillard, Highly photocatalytic activity of nanocrystalline TiO_2 (anatase, rutile) powders prepared from $TiCl_4$by sol–gel method in aqueous solutions, *Process Saf. Environ. Prot.*, 2018, **113**, 109–121, DOI: 10.1016/j.psep.2017.09.006.

31 V. Silva, J. F. A. Fernandes, M. C. Tomas, C. P. Silva., V. Calisto, M. Otero and D. L. D. Lima, Enhanced solar driven photocatalytic removal of antibiotics fromaquaculture effluents by TiO_2/carbon quantum dot composites, *Catal. Today*, 2023, **419**, 114150, DOI: 10.1016/j.cattod.2023.114150.